

Infrared optical absorbance of intersubband transitions in GaN/AlGaN multiple quantum well structures

Qiaoying Zhou, Jiayu Chen, B. Pattada, and M. O. Manasreh^{a)}

Department of Electrical Engineering, 3217 Bell Engineering Center, University of Arkansas, Fayetteville, Arizona 72701

Faxian Xiu, Steve Puntigan, L. He, K. S. Ramaiah, and Hadis Morkoç

Department of Electrical Engineering and Physics Department, Virginia Commonwealth University, Richmond, Virginia 23284

(Received 5 February 2003; accepted 4 April 2003)

Intersubband transitions in Si-doped molecular beam epitaxy grown GaN/AlGaN multiple quantum wells on *c*-plane sapphire were investigated using the Fourier-transform infrared optical absorption technique. Several GaN quantum well samples were grown with either AlGaN bulk or GaN/AlGaN short period superlattice barriers. The measurements were made in a waveguide configuration utilizing a facet polished at 45° to the *c* plane. The integrated area of the intersubband transitions in several waveguides cut from different location of the wafer was measured, from which we estimated the two-dimensional electron gas density (σ). The measured values of σ are about two orders of magnitude larger than the Si doping level of $\sim 8 \times 10^{17} \text{ cm}^{-3}$, which is consistent with the polarization effects, particularly considering the large number of GaN/AlGaN interfaces. The internal quantum efficiency of the intersubband transitions was estimated to be on the order of 40% for samples with superlattice barriers. © 2003 American Institute of Physics.

[DOI: 10.1063/1.1577809]

III-nitride materials have attracted tremendous interest for their applications to ultraviolet, blue/green diode lasers and light-emitting diodes, high-temperature electronics, high-density optical data storage, and electronics for aerospace and automobiles.^{1–3} While most of the applications of III-nitride materials lie in the visible and ultraviolet spectral region, there has been increasing interest in this class of materials for the infrared spectral region.^{4–8} This interest stems from the fact that the GaN/AlGaN system exhibits a large conduction band offset (up to 1.7 eV for the AlN barrier) that allows one to optically design structures with intersubband transitions in the wavelength region spanning 0.7–14 μm . Additionally, the intersubband transition relaxation time in GaN/AlGaN was predicted theoretically^{9–11} to be 100 fs (see also Ref. 8) at 1.55 μm , which is one order of magnitude shorter than the relaxation time in InGaAs multiple quantum wells.¹²

In this paper, we report on the optical absorbance of the intersubband transitions in Si-doped GaN/AlGaN multiple quantum wells grown by molecular beam epitaxy (MBE). The total integrated area of the intersubband transitions was measured. The two-dimensional electron gas (2DEG) density was calculated from the total integrated area and found to be about two orders of magnitude larger than expected from the Si-doping level of $\sim 8 \times 10^{17} \text{ cm}^{-3}$. Thus, the polarization-induced electrostatic charge formed at the GaN/AlGaN interfaces is the dominant factor in the formation of the large 2DEG density in the quantum wells. The internal quantum

efficiency of the intersubband transitions was estimated to be in the order of 40% for most of the samples with superlattice barriers.

The GaN/AlGaN multiple quantum well structures were grown on *c*-plane sapphire (Al_2O_3) substrates using a MBE system with rf plasma N_2 as active nitrogen source. The 2 in. substrate was not rotated during the growth, which resulted in nonuniform growth. An initial AlN buffer layer of ~ 50 nm was grown on nitrated Al_2O_3 substrate as a template for the subsequent epilayers. The growth parameters thus chosen consistently lead to a Ga polarity film. Three wafers denoted A, B, and C were chosen for the present study. The GaN quantum wells in the three samples were doped with $[\text{Si}] \approx 8 \times 10^{17} \text{ cm}^{-3}$. Wafer A consists of a buffer, which is made of 500 Å AlN followed by 0.5 μm GaN, and 50 periods of 35 Å GaN/100 Å $\text{Al}_{0.35}\text{Ga}_{0.65}\text{N}$ multiple quantum wells (MQWs) were grown. A cap layer of 300 Å GaN was then grown at the top of the quantum well structure. Wafer B consists of a buffer layer similar that of sample A and 50 periods of the well/barrier structure. The well is 27.7 Å doped GaN and the barrier is made of four periods of 10 Å Si-doped GaN/15 Å $\text{Al}_{0.65}\text{Ga}_{0.35}\text{N}$. Wafer C consist of a 540 Å AlN and 1.33 μm Si-doped $\text{Al}_{0.50}\text{Ga}_{0.50}\text{N}$ buffer layer followed by 50 periods of well/barrier structure. The well is 13 Å GaN and the barrier consists of four periods of 5 Å Si-doped GaN/10 Å $\text{Al}_{0.65}\text{Ga}_{0.35}\text{N}$. The cap layer of this wafer was 10 Å $\text{Al}_{0.65}\text{Ga}_{0.35}\text{N}$. The optical absorbance measurements were recorded using a BOMEM DA8 spectrometer in conjunction with a continuous flow cryostat. The samples were cut into waveguide geometry with the beveled facet having been polished at 45°. The light beam was zigzagged across the width (*w*) of the sample, which was typically 2.5 mm. The sample thickness (*d*) including the substrate and the

^{a)}Electronic mail: manasreh@engr.uark.edu

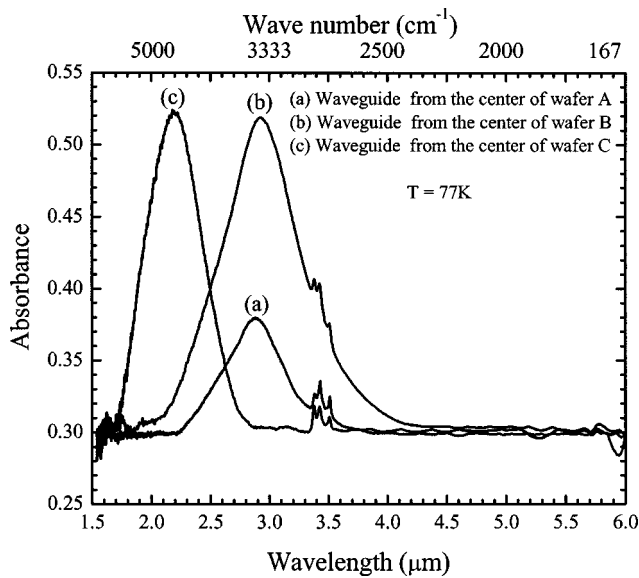


FIG. 1. Absorbance spectra of intersubband transitions measured at 77 K for three waveguides cut from identical locations (center) of GaN/AlGaIn multiple quantum well wafers.

quantum well structure is on the order of 0.43 mm. Thus, the number of passes (P) for the present waveguides is $P = w/[d \times \tan(69.6)] \approx 2$, assuming that the refractive index of the sapphire substrate is 1.7.

In Fig. 1, we show the absorbance of the intersubband transitions as a function of wavelength for the three waveguide samples, which were cut from the center of each of the three wafers. The fine structure observed around $3.4 \mu\text{m}$ is due to C-H local vibrational modes.¹³ The intersubband transition spectra in this figure indicates that the peak position energy is blueshifted toward higher energies as the well width is decreased from 27.7 \AA (sample B) to 13 \AA (sample C). However, the intersubband transition in sample A, which has a well width of 35 \AA , is very close to that of sample B. This indicates that due to the nonuniformity of the wafers, the actual well thickness of both samples A and B is almost the same.

The uniformity of the wafers was investigated by cutting several waveguides from each wafer and then running the absorbance measurements for each waveguide. Some of the results are shown in Fig. 2. The intersubband transition spectra in Fig. 2 were recorded for a sample (cut from the center of wafer B) measured at the Brewster angle configuration [spectrum (a)], and for four waveguides cut from the center [spectra (b) and (c)], middle [spectrum (d)], and edge [spectrum (e)], of wafer B. It is clear from Fig. 2 that the peak position energy of the intersubband transition is almost the same for the waveguides cut from the center of the wafer [see spectra (b) and (c)] but it is blueshifted (shorter wavelength) for the waveguide that was cut halfway between the center and the edge (we refer to this piece as the middle waveguide) of the wafer [see spectrum (d)]. The shift can be explained in terms of the reduction of the well thickness. However, spectrum (e), which was measured for a waveguide that was cut from the edge of the wafer, shows two peaks. This indicates that there are two dominant well thick-

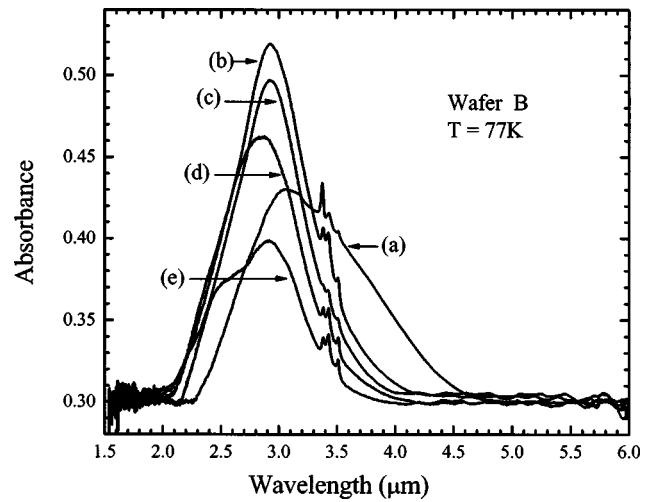


FIG. 2. Several absorbance spectra of intersubband transitions measured for waveguides cut from wafer B. Spectrum (a) was measured at the Brewster angle for a sample cut from the center of the wafer. The remaining spectra were measured for waveguides cut from (b) the center, (c) off center, (d) the middle, and (e) the edge of the wafer. The “middle” is halfway between the center and the edge of the wafer.

nesses of the 50 quantum wells. Moreover, the intensity of the peak is reduced for waveguides cut from the middle and the edge of the wafer. Another observation in Fig. 2 is that the peak position energy of the intersubband transition measured for the waveguides is blueshifted as compared to the peak position energy measured at the Brewster angle. This, however, is opposite to the trend reported for GaAs MQWs,^{14,15} but in agreement with the multiple quantum dot measurements.¹⁶

The total integrated area (I) of the intersubband transition can be related to the 2DEG density (s) according to the following relationship:¹⁷

$$I \approx \frac{PNb\sigma L e^2 h}{4\epsilon_0 m^* c} \frac{f}{n^2(n^2 + 1)^{1/2}}, \quad (1)$$

where P is the number of passes in the waveguide, N is the period of the quantum wells, in this case 50, b is the number of interfaces per period that contribute polarization-induced sheet charges (b is taken as 1 for wafer A and 5 for wafers B and C), σ is the 2DEG density, L is the well thickness, e is the charge of the electron, h is Planck’s constant, ϵ_0 is the permittivity of space, m^* is the electron effective mass, c is the speed of light, n is the refractive index of the quantum well material, and f is the oscillator strength which is taken as $0.96 m_0/m^*$ for the ground state to the first excited state transition.¹⁷ From Eq. (1) one can estimate σ and the results are shown in Table I for the three spectra shown in Fig. 1. Based on the results obtained for the integrated area of the spectra in Fig. 1, we estimated that the integrated area of samples B and C is larger than that of sample A by a factor ~ 4.6 . Hence the value of $b=5$ in Eq. (1) is a good assumption.

The Fermi energy level (E_F) is also estimated using the expression $\sigma_{3D} = 2(2\pi m^* kT/h^2)^{3/2} e^{(E_F - E_c)/kT}$, where k is the Boltzmann constant, T is the temperature, σ_{3D} is the three-dimensional electron density, and E_c is the bottom of

TABLE I. Well width, doping level, 2DEG density estimated from Eq. (1), and Fermi energy level (E_F) with respect to the bottom of the conduction band (E_c) for the samples shown in Fig. 1.

Wafer	Well width (Å)	[Si](10^{11} cm $^{-2}$)	σ (10^{13} cm $^{-2}$)	$(E_F - E_c)$ (eV)	
				77 K	300 K
A	35	2.80	6.93	0.0761	0.244
B	27.7	2.22	5.83	0.0856	0.281
C	13	1.04	15.50	0.0921	0.306

the conduction band. The results are shown in Table I, where $(E_F - E_c)$ is calculated for both 77 and 300 K. From the calculated E_F and the measured intersubband transition energies, it is determined that the Fermi energy level lies between the ground and the first excited states for both 77 and 300 K.

From Table I, it is clear that the Si-doping level cannot alone account for the high 2DEG density estimated from the integrated area of the intersubband transitions. One plausible explanation for the high σ values is that the polarization-induced electrostatic sheet charges at the GaN/AlGaIn interfaces^{18–22} contribute most of the electrons in the well. This premise is supported by the fact that a single interface exists in wafer A (bulk barrier), while there are five interfaces per period (one comes from the quantum well and four come from the superlattice barrier) in wafers B and C. Figure 1 shows clear evidence that the intensity of the intersubband transition for wafer A is much smaller than that of the intersubband transitions in wafers B and C. Hence Eq. (1) was modified by adding the interface factor b .

The internal quantum efficiency η_0 for the three samples was calculated from the absorbance spectra in Fig. 1 according to the following relationship:²³

$$\eta_0 = (I_i - I_{tn})/I_i = [1 - (1 - \zeta)^{NPb}], \quad (2)$$

where I_i is the incident light intensity, $I_{tn} = I_i(1 - \zeta)^{NPb}$, $N=50$, $P=2$, $b=1$ for wafer A and 5 for wafers B and C, and ζ is the fractional absorption per quantum well. ζ is related to the maximum absorbance (A_{\max}) according to the relationship $A_{\max} = -\log_{10}[(1 - \zeta)^{NPb}]$. With the measured values of $A_{\max} = 0.0795$, 0.218, and 0.222 for the three spectra in Fig. 1, one finds $\zeta = 1.823 \times 10^{-3}$, 1.003×10^{-3} , and 1.021×10^{-3} , for spectra (a), (b), and (c), respectively. For these values, the quantum efficiency is calculated to be 16.70%, 39.50%, and 45.40% for the three spectra (a), (b), and (c) in Fig. 1, respectively.

In conclusion, the infrared absorbance measurements of the intersubband transitions in GaN/AlGaIn multiple quantum wells are reported for samples with either bulk or short period superlattice barriers. The two-dimensional electron gas density formed in the quantum wells was estimated from the total integrated area of the intersubband transitions and found to be at least two orders of magnitude larger than the

intentional Si-doping level. The large electron density is attributed to the polarization-induced sheet charges formed at the GaN/AlGaIn interfaces. This assertion was confirmed by the observation of the low (high) value of the integrated area of intersubband transition in samples with AlGaIn bulk (GaN/AlGaIn superlattice) barriers. The internal quantum efficiency was estimated for the intersubband transition, and it was found that samples with superlattice barriers possess higher quantum efficiency as compared to samples with bulk AlGaIn barriers.

The work performed at the University of Arkansas was partially supported by the Air Force Office of Scientific Research (AFOSR) Grant No. F49620-02-1-0299 (Dr. T. Steiner) and the work performed at Virginia Commonwealth University was partially supported by grants from AFOSR (Dr. G. L. Witt and Dr. T. Steiner), the Office of Naval Research (Dr. C. E. C. Wood and Dr. Y. S. Park, and NSF (Dr. Verne Hess and Dr. U. Varshney). The VCU authors would like to thank Dr. M. Reshchikov, Dr. A. Teke, and Dr. F. Yun for their continuing support.

¹H. Morkoç, *Nitride Semiconductors and Devices* (Springer-Verlag, Heidelberg, 1999).

²S. N. Mohammad and H. Morkoç, *Prog. Quantum Electron.* **20**, 361 (1996).

³S. J. Pearton, J. C. Zolper, R. J. Shul, and T. Ren, *J. Appl. Phys.* **86**, 1 (1999).

⁴N. Suzuki and N. Iizuka, *Jpn. J. Appl. Phys., Part 2* **38**, L363 (1999).

⁵C. Gmachl, H. M. Ng, and A. Y. Cho, *Appl. Phys. Lett.* **77**, 334 (2000).

⁶C. Gmachl, H. M. Ng, S.-N. George Chu, and A. Y. Cho, *Appl. Phys. Lett.* **77**, 3722 (2000).

⁷K. Kishino, A. Kikuchi, H. Kanazawa, and T. Tachibana, *Appl. Phys. Lett.* **81**, 1234 (2002).

⁸N. Iizuka, K. Kaneko, and N. Suzuki, *Appl. Phys. Lett.* **81**, 1803 (2002).

⁹N. Suzuki and N. Iizuka, *Jpn. J. Appl. Phys., Part 2* **36**, L1008 (1999).

¹⁰N. Suzuki and N. Iizuka, *Jpn. J. Appl. Phys., Part 2* **37**, L369 (1998).

¹¹N. Suzuki and N. Iizuka, *Proc. SPIE* **3283**, 614 (1998).

¹²T. Asano, K. Tomoda, and S. Noda, in *Extended Abstracts of the 25th International Symposium on Compound Semiconductors*, 1998.

¹³M. O. Manasreh, J. M. Baranowski, K. Pakula, H. X. Jiang, and Jingyu Lin, *Appl. Phys. Lett.* **75**, 659 (1999).

¹⁴E. Dupont, M. Gao, H. C. Liu, Z. R. Wasilewski, A. Shen, M. Zaluzny, S. R. Schmidt, and A. Seilmeier, *Phys. Rev. B* **61**, 13 050 (2000).

¹⁵M. Zaluzny and C. Nalewajko, *Phys. Rev. B* **59**, 13 043 (1999).

¹⁶B. Pattada, Jiayu Chen, M. O. Manasreh, M. Hussien, W. Ma, and G. J. Salamo, *Appl. Phys. Lett.* **82**, 2509 (2003).

¹⁷L. C. West, S. J. Eglash, *Appl. Phys. Lett.* **46**, 1156 (1985).

¹⁸F. Bernardini, V. Fiorentini, and D. Vanderbilt, *Phys. Rev. B* **56**, R10 024 (1997).

¹⁹E. T. Yu, G. J. Sullivan, P. M. Asbeck, C. D. Wang, D. Qiao, and S. S. Lau, *Appl. Phys. Lett.* **71**, 2794 (1997).

²⁰E. T. Yu, in *III-V Nitride Semiconductors: Applications and Devices*, Vol. 19, edited by E. T. Yu and M. O. Manasreh (Taylor and Francis, New York, 2003), Chap. 4, pp. 161–191.

²¹H. Morkoç, R. Cingolani, and Bernard Gil, *Innovations Mater. Res.* **3**, 97 (1999).

²²H. Morkoç, A. Di Carlo, and R. Cingolani, *Solid-State Electron.* **46**, 157 (2002).

²³E. R. Brown, S. J. English, and K. A. McIntosh, in *Long Wavelength Infrared Detectors*, Vol. 1, edited by M. Razeghi (Gordon and Breach, Amsterdam, 1996), Chap. 6, p. 335.